

Weighing Super-Massive Black Holes with Narrow Fe K α Line

Peng Jiang, Junxian Wang and Xinwen Shu

*CAS Key Laboratory for Research in Galaxies and Cosmology, Department of Astronomy,
University of Science and Technology of China, Hefei, Anhui 230026, China*

jpaty@mail.ustc.edu.cn

ABSTRACT

It has been suggested that the narrow cores of the Fe K α emission lines in Active Galactic Nuclei (AGNs) are likely produced in the torus, the inner radius of which can be measured by observing the lag time between the V and K band flux variations. In this paper, we compare the virial products of the infrared time lags, and the narrow Fe K α widths for 10 type 1 AGNs, with the black hole masses from other techniques. We found the narrow Fe K α line width is in average $2.6^{+0.9}_{-0.4}$ times broader than expected, assuming an isotropic velocity distribution of the torus at the distance measured by the infrared lags. We propose the thick disk model of the torus may explain the observed larger line width. Another possibility is the contamination by emission from the broad line region or the outer accretion disk. Alternatively, the narrow iron line might originate from the inner most part of the obscuring torus within the sublimation radius, while the infrared emission may be from the outer cooler part. We note the correlations between the black hole masses based on this new technique and those based on other known techniques are statistically insignificant. We argue that this could be attributed to the small sample size and the very large uncertainties in the measurements of iron K line widths. The next generation of X-ray observatories could help verify the origin of the narrow iron K α line and the reliability of this new technique.

Subject headings: black hole physics – galaxies: active – galaxies: nuclei – galaxies: Seyfert – X-rays: galaxies – infrared: galaxies

1. INTRODUCTION

Under the unified scheme of Active Galactic Nuclei (AGNs), Seyfert 1 nuclei with broad line regions (BLRs) would be classified as Seyfert 2 if the BLRs were obscured by encircling

dust tori [1]. As nearly all of the parsec-sized dust tori can not be spatially resolved (note that Jaffe et al. reported interferometric mid-infrared observations that spatially resolve the dust torus in NGC 1068 [2]), the size and geometry of torus are not well understood. Recent researches measured the inner radius of dust torus by observing the time-delayed responses of the K band flux variations to the V band flux variations, as the bulk of the K band flux should originate in the thermal radiation of hot dust surrounding the central engine [3,4,5].

The iron $K\alpha$ emission line at ~ 6.4 keV was first identified as a common feature in the X-ray spectrum of AGNs by *Ginga* [6,7]. The line can be promptly interpreted as fluorescence emission following photoelectric absorption of the hard X-ray continuum [8]. Recent *XMM-Newton* and *Chandra* observations revealed narrow (unresolved by *XMM*) iron $K\alpha$ lines at ~ 6.4 keV in the X-ray spectra of most AGNs [9,10,11]. However, the origin of the narrow iron $K\alpha$ line is still poorly understood. Possible origins of the narrow line include the outermost regions of the accretion disk, the BLR, and the dust torus. Nandra found that the average Fe $K\alpha$ core emission width in a sample of type 1 AGNs is about a factor of two narrower than the broad emission line width (specifically $H\beta$), and there is no correlation between them [12]. This suggests that the iron $K\alpha$ emission lines are likely, in many cases, originated in the torus at larger scales but not the BLRs.

Reverberation mapping [13,14] of BLRs is one of few methods that can directly derive the masses of super-massive black holes (SMBHs) in AGNs. In tracing the response of the gas in BLRs to the variable ionizing continuum of AGNs, the time delay between the variations in the continuum and the broad emission lines gives a characteristic radius of the BLR gas. With the orbital velocity estimate based on the width of the broad emission line, the black hole masses can be derived as:

$$M_{BH} = f \frac{c\tau V^2}{G} \quad (1)$$

The scaling factor f is determined by the geometry and velocity distribution of the BLR gas. One of the uncertainties in this technique is that the geometry and velocity distribution of the BLR is unknown, and independent techniques are required to test and calibrate the derived black hole masses. Another technique to weigh SMBHs in AGNs is based on the tight relationship between the SMBH mass and the velocity dispersion of the bulge or spheroid [15,16]. The $M_{BH} - \sigma_*$ relationship was primarily discovered in quiescent galaxies; however, recent studies have suggested that active SMBHs have the same correlation [17,18,19].

In this paper we compare the virial products of the infrared time lags and the narrow Fe $K\alpha$ widths for 10 type 1 AGNs with the black hole masses from other techniques. Such study can put strong constraints on the origin of the narrow Fe $K\alpha$ line.

2. DATA AND RESULTS

We search for archival *Chandra* HETG observations for AGNs, as *Chandra* is the only instrument currently capable of resolving narrow iron $K\alpha$ lines. We only choose the objects with narrow Fe $K\alpha$ lines detected at a confidence level $> 3\sigma$. We also restrict our sample with BLR reverberation mapping data available. The resulting sample consists of ten Seyfert 1 galaxies. All the archival *Chandra* HETG observations of these AGNs are listed in Table 1. The process of data reduction and spectrum fitting is described in [11]. To improve the measurement of line widths, for sources with more than one HETG exposure, we fitted multiple spectra simultaneously with invariable line center energy and FWHM. The fitting results are shown in Table 2.

From literature, we find infrared time lags for six of the sources (see table 2). From Fig. 30 in [4], we see a tight correlation between the infrared lag and the V band luminosity, with a scatter of 0.2 dex. Such a relationship was adopted to estimate the infrared lags for the remaining four sources without infrared reverberation mapping observations in our sample.

Peterson et al. presented black hole masses for 35 AGNs based on broad emission-line reverberation mapping data [20]. The black hole masses are derived as

$$M_B = \frac{f_B c \tau \sigma_{line}^2}{G}, f_B = 5.5 \quad (2)$$

where f_B (the scaling factor for BLR reverberation mapping) is a zero-point calibration determined using the $M_{BH} - \sigma_*$ relationship [19,24,25].

Since the narrow Fe $K\alpha$ line is always modeled by a single Gaussian component, in this research we calculate the virial products as

$$M_T = \frac{f_T c \tau V_{FWHM}^2}{4G} \quad (3)$$

where f_T is the scaling factor, τ the infrared lag and V_{FWHM} the FWHM of the narrow iron $K\alpha$ line. For a Gaussian, $FWHM/\sigma_{line} = 2.355$. Note although the Fe $K\alpha$ line consists of two components ($K\alpha_1$ and $K\alpha_2$), with the spectral resolution of the HETG, its impact on the measurement of the line width with a single Gaussian is negligible [26].

As shown in Figure 1, nine of the derived M_T s are consistent with M_{BS} , but a scaling factor is required. The solid line is the best-fit line (slope fixed to 1) for all ten sources, derived using the orthogonal regression program GAUSSFIT (version 3.55; [27]). The asymmetric statistical errors in the masses were symmetrized as the mean of the positive and negative errors since GAUSSFIT can not work with asymmetric errors. The best-fit scaling factor f_T is 0.44 ± 0.19 . While excluding the outlier NGC 5548, the best-fit value is $f_T = 0.35 \pm 0.10$.

However, we note the correlation between M_T and M_B is insignificant. The Spearman’s correlation test yields a confidence level of only 86.5% ($\rho = 0.528$), even after excluding NGC 5548.

In Figure 2, M_T/f_T is plotted versus σ_* for seven sources with σ_* available in literature (see Table 2). A best-fit was made to the filled points

$$\log\left(\frac{M_T}{f_T}\right) = \alpha + \beta \log\left(\frac{\sigma_*}{200}\right) \quad (4)$$

where we adopt $\alpha = 8.13 \pm 0.06$ and $\beta = 4.02$ as reported by Tremaine et al. for quiescent galaxies [28]. The best-fit yields a scaling factor f_T of 0.42 ± 0.23 . While excluding NGC 5548, we obtained $f_T = 0.29 \pm 0.11$, and a confidence of the correlation of 83.3% (Spearman’s $\rho = 0.617$).

3. DISCUSSION

Assuming a torus origin of the narrow Fe K α line, we obtained the virial products of the narrow iron K α widths and the infrared time lags for 10 Seyfert 1 galaxies. We found nine out of ten derived virial masses were consistent with those masses measured based on reverberation mapping of optical broad emission lines [20]; however, a scaling factor ~ 0.4 is required. For seven sources with σ_* measurements, six of them showed virial masses consistent with the M - σ_* relationship, assuming a similar scaling factor ~ 0.4 .

The most common assumption for converting a virial product to M_{BH} is:

$$M_{BH} = \frac{3rV_{FWHM}^2}{4G}, \quad (5)$$

which implicitly assumes an isotropic velocity distribution [29]. The scaling factor we obtained indicates that the narrow Fe K α core is in average $2.6^{+0.9}_{-0.4}$ times broader than expected assuming an isotropic velocity distribution of the torus at the distance measured by the infrared lags.

One possible explanation is that the narrow iron K α line originates from smaller radius than the infrared radiation does. For instance, the obscuring torus might span a large range of scale; the narrow iron K α line originates from a smaller scale where the temperature is too high and dust does not exist, while the infrared radiation comes from a larger scale with lower temperatures. Alternatively, the narrow iron K α line might be contaminated by the BLR/disk component, thus causing the line width of the torus component to be overestimated. If this is true, we would expect a variation of the narrow Fe K α line at time

scales ~ 6.8 times smaller than the infrared lags. We note rapid variations of the narrow Fe K α line has been reported in NGC 7314 [30] and Mrk 841 [31] but not detected in other sources.

Another possibility is that the velocity distribution for dust torus might not be virial. Here, we consider the dust torus as a thick disk [32]. The thick disk would be sustained vertically by a pressure which is most probably provided by turbulence with a characteristic velocity H/RV_K , where R is the radius from the central black hole at the equator and V_K is the local Keplerian velocity at R . Thus, the observed value of V_{FWHM} is given by

$$V_{FWHM} \approx 2V_K \sqrt{(H/R)^2 + \sin^2 i} \quad (6)$$

where i is the inclination of the equator to our line of sight. The observed mass (virial product without any scaling factor) is:

$$M_{obs} = \frac{c\tau V_{FWHM}^2}{4G} \quad (7)$$

$$M_{obs} = ((H/R)^2 + \sin^2 i) \frac{c\tau V_K^2}{G} \quad (8)$$

$$M_{obs} = ((H/R)^2 + \sin^2 i) M_T \quad (9)$$

Hence,

$$f_T = \frac{1}{(H/R)^2 + \sin^2 i} \quad (10)$$

The observed ratio of Seyfert 2 to Seyfert 1 galaxies of about 4 [33] would imply a relative torus thickness of $H/R \approx 1.33$, if the distinction is solely due to the orientation of the torus. Thus a scaling factor < 1 is plausible under this scheme. It is also clear from the last equation that f_T is less sensitive to the inclination for $H/R > 1$. This suggests that if this model for the narrow Fe K α line can be confirmed, the narrow Fe K α line could be used as a good tool to weigh the central SMBH since it is insensitive to the inclination.

In both Fig. 1 and Fig. 2, the only outlier NGC 5548 shows an relatively underestimated M_T . Cackett & Horne analyzed 13 years results of optical spectrophotometric monitoring of the NGC5548 and gave a luminosity-dependent model of BLRs to explain the variable width of H β lines and its variable time-delayed lags [34]. It is possible that the size of torus also varies with luminosity in this source. We note that the narrow iron K α line width varied significantly between two individual exposures; from 5090_{-2030}^{+2020} km s $^{-1}$ in 2000 to 1690_{-1690}^{+1290} km s $^{-1}$ in 2002. The line intensity also decreased from $3.4_{-1.1}^{+1.5} \times 10^{-5}$ photons cm $^{-2}$ s $^{-1}$ to $2.2_{-0.7}^{+0.6} \times 10^{-5}$ photons cm $^{-2}$ s $^{-1}$. Meanwhile the continuum luminosity (2.0 – 10.0 keV) increased from 1.5×10^{43} ergs s $^{-1}$ to 1.9×10^{43} ergs s $^{-1}$. This suggests a variable

origin of the narrow iron $K\alpha$ line. The line width presented in Table 2 is dominated by the second observation with longer exposure time. If simply taking the line width from the first exposure, we can obtain a black hole mass four times higher, well consistent with the best-fit lines in Fig. 1 and 2. For the remaining sources with multiple available HETG exposures, no narrow iron $K\alpha$ line variation was found to be significant.

While the correlation between M_T and M_B is statistically insignificant (at a confidence level of 87% excluding NGC 5548), we argue that this may be attributed to the large uncertainties in the measurements of M_T because of the large errorbars in the iron K line widths. In Fig. 1 and 2 we can see that the large scattering of data points from the best-fit lines are mainly due to the large uncertainties in the measurements of iron $K\alpha$ line width. The scattering of data points in Fig. 1 can be measured by the standard deviation of $\log(M_T/M_B)$, which is 0.50 for ten sources and 0.38 with NGC 5548 excluded. This is comparable to the typical 1σ uncertainty of $\log(M_T/f_T)$ which is ~ 0.35 .

To verify the reliability of this new technique to weigh SMBH, more data points and better measurements of iron $K\alpha$ line widths are required. Given the difficulty in obtaining lengthily HETG observations with the required S/N to constrain the iron line width, we have to await the next generation of X-ray observatories that are able to measure the iron K line at higher spectral resolutions (i.e. of the order 100 km/s) with calorimeter-based detectors. Before that, we need future X-ray observations to verify the origins of the narrow iron $K\alpha$ line by better resolving the line profile and X-ray reverberation-mapping.

The work is supported by The Chinese NSF through NSFC10773010 and NSFC 10825312. We would like to thank Dr. Wei Zheng for helpful comments and his careful review of the manuscript. JXW thanks Dr. Tinggui Wang and Matt Malkan for discussions. Jiang acknowledges support from the "Chuang Xin" Foundation operated by the Graduate School of USTC.

REFERENCES

- Antonucci, R. 1993, ARA&A, 31, 473
- Beckert, T., & Duschl, W. J. 2004, MNRAS, 426, 445
- Blandford, R., & McKee, C. F. 1982, ApJ, 255, 419
- Cackett, E. M., & Horne, K. 2006, MNRAS, 365, 1180
- Clavel, J., Wamsteker, W., and Glass, I. S. 1989, ApJ, 337, 236

- Ferrarese, L., & Merritt, D. 2000, *ApJ*, 539, L9
- Ferrarese, L., Pogge, R. W., Peterson, B. M., Merritt, D., Wandel, A., and Joseph, C. L. 2001, *ApJ*, 555, L79
- Gebhardt, K., et al. 2000, *ApJ*, 539, L13
- Glass, I. S. 1992, *MNRAS*, 256, 23
- Haehnelt, M. G., & Kauffmann, G. 2000, *MNRAS*, 318, L35
- Jaffe, W. et al. 2004, *Nature*, 429, 47
- Jefferys, W. H., Fitzpatrick, M. J., and McArthur, B. E. 1988, *Celestial Mechanics*, 41, 39
- Jiang, P., Wang, J. X., and Wang, T. G. 2006, *ApJ*, 644, 725
- Maiolino, R., & Rieke, G. H. 1995, *ApJ*, 271, L7
- Minezaki, T., Yoshii, Y., Kobayashi, Y., Enya, K., Suganuma, M., Tomita, H., Aoki, T., and Peterson, B. A. 2004, *ApJ*, 600, L35
- Nandra, K. 2006, *MNRAS*, 368, 62
- Nandra, K., & Pounds, K.A. 1994, *MNRAS*, 268, 558
- Nelson, C. H. 1996, *ApJ*, 465, L87
- Netzer, H. 1990, in *Active Galactic Nuclei*, ed. R. D. Blandford, H. Netzer, & L. Woltjer (Berlin: Springer), 137
- Onken, C. A., Peterson, B. M., Dietrich, M., Robinson, A., and Salamanca, I. M. 2003, *ApJ*, 585, 121
- Onken, C. A., Ferrarese, L., Merritt, D., Peterson, B. M., Pogge, R. W., Vestergaard, M., and Wandel, A. 2004, *ApJ*, 615, 645
- Page, K. L., O’Brien, P. T., Reeves, J. N., and Turner, M. J. L. 2004, *MNRAS*, 347, 316
- Peterson, B. M. 1993, *PASP*, 105, 247
- Peterson, B. M., Ferrarese, L., Gilbert, K. M., Kaspi, S., Malkan, M. A., Maoz, D., Merritt, D., Netzer, H., Onken, C. A., Pogge, R. W., Vestergaard, M., and Wandel, A. 2004, *ApJ*, 613, 682
- Petrucchi, P. O., et al. 2002, *A&A*, 388, L5
- Pounds, K. A. et al. 1990, *Nature*, 344, 132
- Reynolds, C. S., & Nowak, M. A. 2003, *Phys. Repl.*, 377, 389
- Silk, J., & Rees, M. J. 1998, *MNRAS*, 331, L1

- Suganuma, M., Yoshii, Y., Kobayashi, Y., Minezaki, T., Enya, K., Tomita, H., Aoki, T., Koshida, S., and Peterson, B., A. 2004, ApJ, 612, 113
- 2006, ApJ, 639, 46
- Tremaine, S., et al. 2002, ApJ, 574, 740
- Yaqoob, T., George, I. M., Nandra, K., Turner, T. J., Serlemitsos, P. J., and Mushotzky, R. F. 2001, ApJ, 546, 759
- Yaqoob, T., George, I. M., Kallman, T. R., Padmanabhan, U., Weaver, K. A., and Turner, T. J. 2003, ApJ, 596, 85Y
- Yaqoob, T., & Padmanabhan, U. 2004, ApJ, 604, 63Y

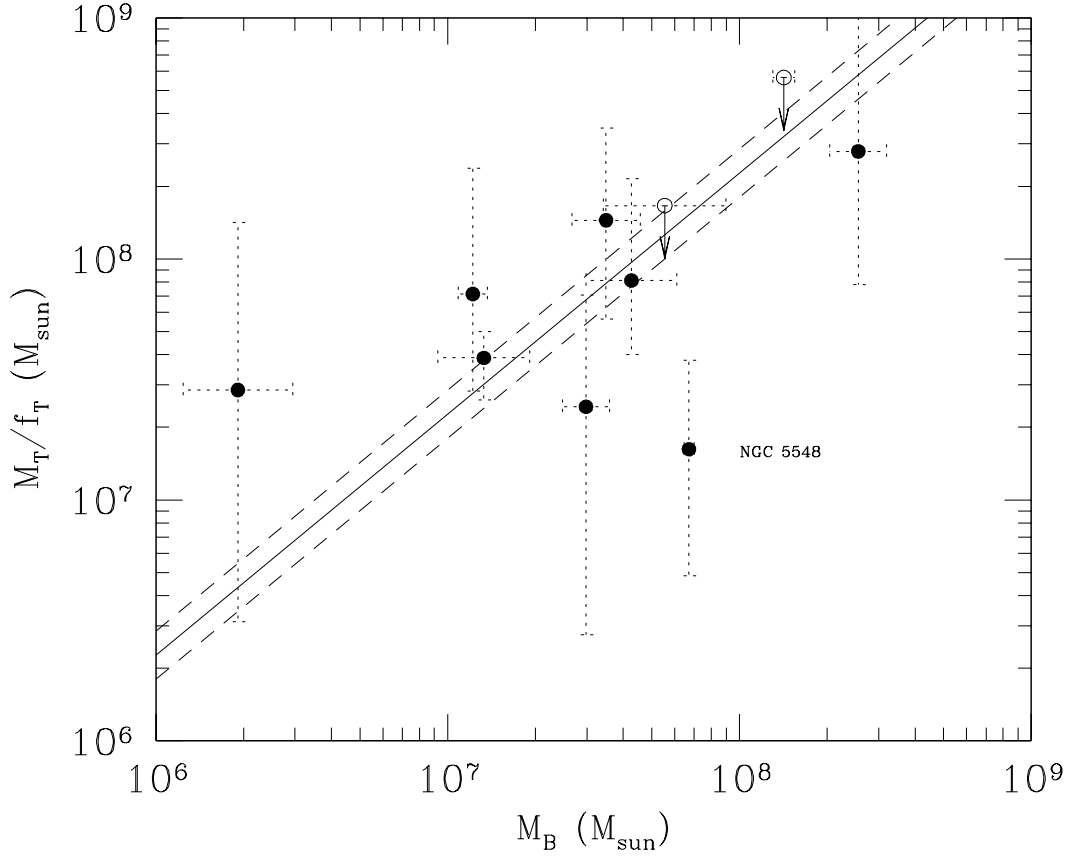


Fig. 1.— M_T/f_T is plotted versus M_B . The data are presented in Table 2. The solid line is the best-fitting line by fixing the slope at 1. The dashed lines give the scatter in the normalization.

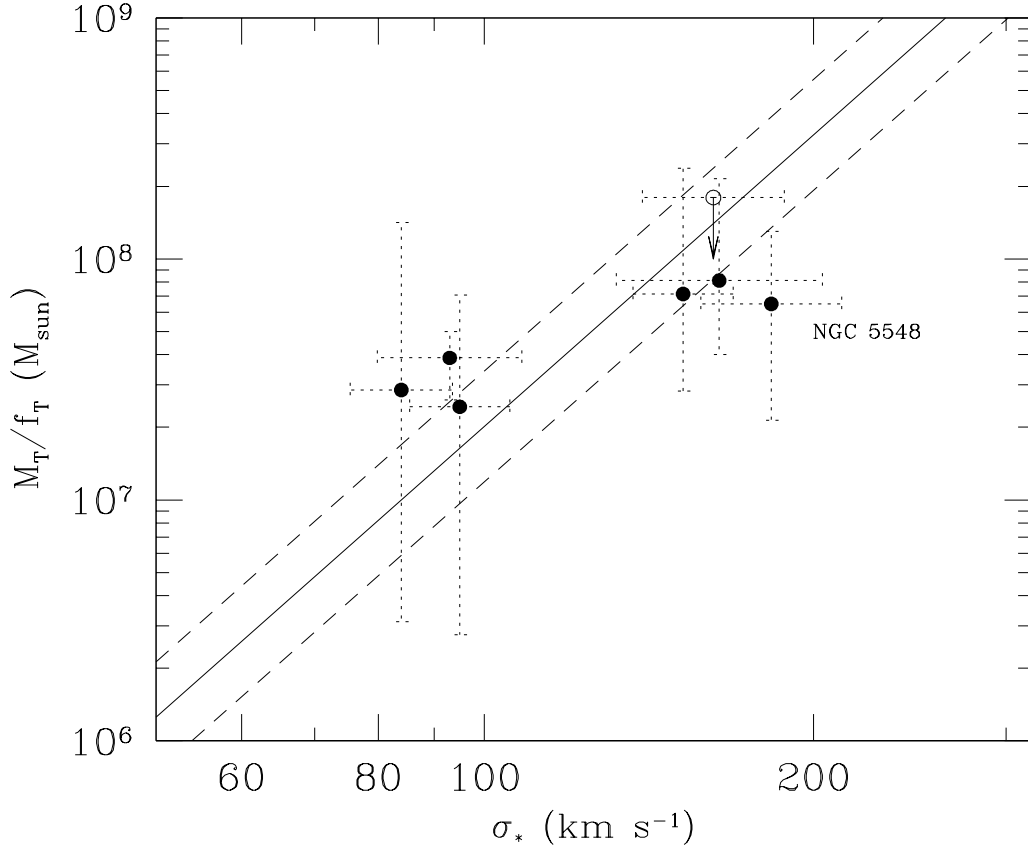


Fig. 2.— M_T/f_T is plotted versus σ_* . The solid line is the best-fitting line by fixing the slope at 1. The dashed lines give the scatter in the normalization. Data are presented in Table 2.

Table 1. *Chandra* HETG Observations

Object	Start date	Exposure time (ksec)
NGC 4051	2000-03-24	80.79
NGC 4151	2000-03-05	48.03
	2002-05-07	92.89
	2002-05-09	156.60
NGC 3783	2000-01-20	57.16
	2001-02-24	167.78
	2001-02-27	171.01
	2001-03-10	167.57
	2001-03-31	168.20
	2001-06-26	168.30
NGC 7469	2002-12-12	79.89
	2002-12-13	69.76
Fairall 9	2001-09-11	79.94
NGC 5548	2000-02-05	82.32
	2002-01-16	153.9
NGC 3516	2001-04-09	36.16
	2001-04-10	74.54
	2001-11-11	89.45
MKN 279	2002-05-18	116.06
MKN 509	2001-04-13	58.69
3C 120	2001-12-21	58.16

Table 2. Estimates of Black Hole Masses of Ten Seyfert 1 Galaxies

Object	FWHM (km s ⁻¹)	τ_{IR} (days)	$\log (M_T/f_T)$ (M_\odot)	$\log M_B$ (M_\odot)	σ_* (km s ⁻¹)	References
NGC 4051	6160 ⁺⁴⁷¹⁰ ₋₂₉₈₀	15.4±9.1	7.456 ^{+0.695} _{-0.962}	6.281±0.188	84±9	4, 11, 19, 20
NGC 4151	4070 ⁺⁴⁵⁰ ₋₆₃₀	48.0 ⁺² ₋₃	7.589 ^{+0.109} _{-0.174}	7.124±0.157	93±14	19, 20, 22
NGC 3783	2420 ⁺¹⁵⁹⁰ ₋₁₅₈₀	85.0±5	7.386 ^{+0.463} _{-0.945}	7.474±0.080	95±10	11, 19, 20, 23
NGC 7469	4540 ⁺²⁸⁵⁰ ₋₁₂₃₀	70.9±18	7.854 ^{+0.521} _{-0.402}	7.086±0.050	152±16	4, 19, 20
Fairall 9	3780 ⁺³⁴⁶⁰ ₋₁₄₇₀	400.0±100	8.446 ^{+0.661} _{-0.553}	8.407±0.097		11, 20, 21
NGC 5548	2540 ⁺¹¹⁷⁰ ₋₁₀₈₀	51.4±4.9	7.210 ^{+0.369} _{-0.524}	7.827±0.017	183±27	4, 19, 20
NGC 3516	4320 ⁺²⁷⁰⁰ ₋₁₂₉₀	89.1	7.910 ^{+0.422} _{-0.308}	7.630±0.155	164±35	11, 19, 20
MKN 279	5240 ⁺²⁸⁹⁰ ₋₁₉₇₀	109.6	8.160 ^{+0.382} _{-0.410}	7.543±0.117		11, 20
MKN 509	< 6550	269.2	< 8.752	8.152±0.037		1, 6, 7
3C 120	< 3810	234.4	< 8.221	7.744±0.210	162±24	11, 19, 20

Note. — The widths of iron line were reported in the source rest frame. Statistical errors for line widths and $\log(M_T/f_T)$ are 90% confidence. For the rest quantities, 1σ uncertainties are adopted from literature. For NGC 4051, NGC 7469 and NGC 5548, we reported the average IR lags observed during the period 2001–2003. For NGC 3516, MKN 279, MKN 509 and 3C 120, the IR lags were estimated based on the relationship $\Delta t \propto L^{0.5}$.